IET Energy Systems Integration

国家电网
STATE GRID
中国电力科学研究院有限公司
CHINA ELECTRIC POWER RESEARCH INSTITUTE

IET The Institution of
Engineering and Technology WILEY

ORIGINAL RESEARCH PAPER

Modelling and control of district heating networks with reduced pump utilisation

Hector Bastida | Carlos E. Ugalde-Loo ⬤ | Muditha Abyesekera | Meysam Qadrdan

School of Engineering, Cardiff University, Cardiff, Wales, UK

Correspondence

Carlos E. Ugalde-Loo, School of Engineering, Cardiff University, Queen's Buildings, The Parade, CF24 3AA, Cardiff, Wales, UK.
Email: Ugalde-LooC@cardiff.ac.uk

Abstract

District heating systems (DHS) provide thermal energy to a range of consumers. Hence, an adequate sizing of the key elements involved in the energy supply system and their management are critical. Pumps and valves are essential components of a DHS as they ensure hydraulic operating conditions are met for the energy distribution process. To achieve this, a hydraulic system is typically controlled by defining a differential pressure set-point at a critical location in the network. However, a good understanding of the dynamic behaviour of the hydraulic system during the diverse operating conditions is required for its efficient control and to maximise its performance. This paper presents a control strategy based on suitable dynamic models of the hydraulic system. These non-linear models enable the simulation of the behaviour of mass flow rate, pressure drops in pipes, power consumption of the pump and the heat delivery to meet the thermal loads. Control system design is carried out in MATLAB, and the designed controller is verified with Apros—a commercial process simulation software. It is shown that the hydraulic behaviour of a DHS is well described by the dynamic models presented. In addition, the designed control scheme reduces the electricity consumption of pumps compared with a conventional mass flow rate controller based on a look-up table and a differential pressure valve.

1 | INTRODUCTION

District heating and cooling systems (DHCSs) are widely used for the supply of space heating and cooling to buildings. A DHCS comprises the heat and cooling sources, distribution pipe networks and consumer heat substations [1]. It can be considered an integrated energy system as different energy vectors such as electricity, heating and cooling are linked together by coupling technologies. For example, a gas-fired combined heat and power unit is a coupling element between electricity, heat and gas systems.

Heating and cooling supply processes in a DHCS require an effective performance of different components to ensure consumer demand is met under a range of operating conditions. Typically, energy management is carried out by local controllers working independently from each other [2]. The actuators governed by different control strategies act over key variables of the DHCS (i.e. temperature, mass flow rate and differential pressure) to meet heating and cooling demands.

Thus, the controllers' set-points need to be modified according to the energy demand profile.

Different approaches have been used to assess and increase the efficiency of the energy transportation process of hydraulic networks in a DHCSs. For example, system performance can be optimised using a synchronised schedule for all energy sources [3]. Alternatively, the operation of a pipe network to transport hot or cold water could be improved to reduce the electrical power consumption of the pumps. To achieve this, the hydraulic behaviour of the DHCS is assessed so that effective controllers are designed to ensure adequate hydraulic operating conditions and to guarantee that the energy demand is met. For instance, the modelling approach presented in Ref. [4] uses a resistance ratio to predict the hydraulic behaviour of a pipe network. However, the practical use of this methodology is limited as it would require several sensors to measure differential pressures throughout the network so that correction factors are accurately calculated.

Other references found in the literature focus on the regulation of mass flow rate in pipe networks so that the

energy supplied is modified and the heating and/or cooling production is reduced. The method reported in Refs [5,6] is based on the mathematical model of an economical friction factor, with a variable-speed pump configuration being used. However, the non-linear behaviour of the pump's efficiency is not considered. An iterative method to achieve hydraulic balance based on a genetic algorithm is presented in Ref. [7]. Nevertheless, the temperature dependence on the pipe friction factor, a crucial parameter affecting the hydraulic behaviour of a pipe network, is not accounted. Likewise, an iterative method for the balancing of pipe networks is used in Refs [8–10]. Based on the principle of conservation of energy, this analytical method defines the energy losses for each element in the network. However, the temperature changes inside the pipes are neglected—even though they are critical to calculate the energy supply in each pipe branch.

Hybrid models including conventional central circulating and distributed variable-speed pump topologies are presented in Refs [11,12]. Control strategies to optimise pipeline pressures are used to minimise the total power consumption of the pumps. Although these references present methods to model, control and optimise the hydraulic performance of a DHCS, they are based on steady-state or quasi-steady-state approximations. These hybrid models require a large computational time since iterative methods are used to find system parameters for specific operating points. Furthermore, their accuracy is limited by assumptions aimed to simplify the complexity of the solving method, such as a constant friction factor or the lack of temperature dependence.

The use of steady- or quasi-steady-state models prevents the comprehensive analysis of pipe networks including not only the hydraulic, but also the thermal behaviour [13–20]. For example, quasi-steady-state models include variations on the operating conditions but do not consider transient responses of critical thermal and hydraulic variables. To be able to maximise the dynamic performance of a DHCS, temperature and pressure drop should be also considered in the analysis. On the one hand, dynamic simulations allow the analysis of operating conditions and their effects over system components, such as heat supply substations. On the other hand, adequate models capable of capturing the accurate dynamic behaviour of the system are necessary to develop efficient control systems.

To address the aforementioned shortcomings, the objective of this study is to develop a hydraulic dynamic model for a pipe network of a district heating system (DHS) suitable for control system design. The presented dynamic modelling approach goes beyond steady- and quasi-steady-state regimes and considers pipe parameters such as the friction factor and the relative roughness, which ensures a higher accuracy. Physical principles are used to develop the model considering the non-linearity of the elements of the pipe network. Thus, non-linear differential equations are obtained. This way, rates of change of temperature, differential pressure and mass flow are modelled under different operating conditions.

To illustrate the modelling approach, the mathematical model of a simple pipe network is developed, from first principles, and implemented in MATLAB. To provide confidence in the modelling methodology, the model is then verified using Apros (an advanced process commercial simulation software). Although Apros has a number of libraries with components for energy systems and industrial processes [21–23], it is not suitable for control system design, which is instead carried out using MATLAB. To further demonstrate the capabilities of the modelling technique, a more representative DHS model is built in MATLAB. This is, in turn, linearised to design simple proportional-integral (PI) controllers using frequency response tools. Finally, the DHS, together with relevant controllers, is implemented in Apros to verify the system operation using commercial software. Simulation results show that it is possible to reduce the electricity consumption of the pump whilst hydraulic operating conditions and energy supply demands are met.

Note: Although the focus of this study is on DHS, the modelling approach presented here may be also adopted for district cooling systems (DCS) or DHCS.

2 | MATHEMATICAL MODELS

The dynamic behaviour of a network transporting a fluid is characterised by its high non-linearity. Despite their inherent complexity, accurate dynamic models are essential to design adequate controllers. In this section, mathematical models of the main components of a pipe network in a DHS are presented.

2.1 | Pump model

Due to the complexity of the flow through a centrifugal pump, its hydraulic behaviour cannot be described accurately by an equation based on fluid mechanics theory [24]. The performance of a pump is instead determined experimentally through tests and described by a set of curves. Usually, these curves are provided by manufacturers and represent the relation between volumetric flow (Q) or mean velocity (v) and the head (h) produced at a specific pump speed. Therefore, h is determined by the speed of the engine (ω) and the generated fluid velocity. Assuming a steady and incompressible flow, neglecting friction effects and by applying Bernoulli's equation through the input and output of the pump, the relationship between the head produced by the pump and its pressure drop is given by Ref. [24].

$$\Delta p = \rho g h = f(\omega, v), \tag{1}$$

where ρ is the density of the fluid, g is the gravitational acceleration and Δp is the pressure boost between the inlet and outlet of the pump.

A set of efficiency curves can be simplified using the nominal efficiency curve (see Figure 1). By using the affinity laws of pumps [24], the relationship between the efficiency

curve at nominal speed (ω_N) and any given pump speed (ω_x) is provided by

$$\frac{h_N}{h_x} = \frac{\omega_N^2}{\omega_x^2} \tag{2}$$

The head produced for any speed set-point can be described by a polynomial equation as

$$h = P_1 Q^2 + P_2 Q \omega_{sp} + P_3 \omega_{sp}^2 \tag{3}$$

where ω_{sp} is the set-point of the motor speed of the pump (defined as a value between 0 and 1), and P_1, P_2, and P_3 are the coefficients of the polynomial equation, which can be calculated via linear regression using the given pump curve. The volumetric flow is defined in terms of mean velocity, with $Q = 3600\,Av$, where A is the flow area of the pump. The pressure boost between the inlet and the output of the pump may be calculated using Equation (1).

The pump's power consumption is determined by its motor efficiency (η_m), its hydraulic efficiency (η), ρ, Q, and h as

$$P = \frac{\rho g Q h}{\eta \eta_m} \tag{4}$$

2.2 | Pipe hydraulic model

The pressure drop in a pipe is dependent on the wall shear stress (τ). The laminar shear stress is defined by $\tau_{\text{lam}} = \mu u$, where μ is the dynamic viscosity and u is the velocity of the fluid. However, unlike laminar flows, turbulent flows exhibit random fluctuations of velocity components in all directions within the fluid. This behaviour increases the transport of momentum. The turbulent shear stress is defined by

$\tau_{\text{turb}} = \rho \overline{uv}$, where ρ is the fluid density, u is the velocity of the fluid, v is the rate of mass transfer of the fluid and the overbar denotes a mean value [24]. Thus, for turbulent flows, τ is a function of density which, in turn, is temperature dependent. This implies that the movement of the fluid through the pipe is affected by τ. The friction factor (f), in turn, describes the relation between the velocity of the fluid and τ. Its calculation depends on the Reynolds number (Re) of the fluid, the relative roughness of the pipe (ε) and the diameter of the pipe (D), with $f = \varphi(\text{Re}, \varepsilon/D)$.

The pipe friction factor is calculated using analytical equations. It is defined by two ranges: laminar (no dependence on density) and turbulent. The transient region between both ranges is not considered. For $320 < \text{Re} < 2100$ (laminar flow), f is given by

$$f = \frac{64}{\text{Re}}, \tag{5}$$

and for values between 5000 and 1×10^8 (turbulent flow), f is calculated using [25]:

$$f = 0.25 \left/ \left[\log\left(\frac{\varepsilon/D}{3.71} + \frac{5.74}{\text{Re}^{0.9}} \right) \right]^2 \right. . \tag{6}$$

The total pressure drop (Δp) in a pipe is calculated by applying the energy conservation principle for a steady incompressible flow. This considers the effect of friction previously described along the streamline that passes through the length of the pipe and uses the Darcy–Weisbach equation to consider the major head losses in the pipe. This way, Δp is defined as [24].

$$\Delta p = f \frac{L_{eq} \rho v^2}{2D}, \tag{7}$$

where L_{eq} is the equivalent length of the pipe. As it can be observed from Equation (7), pressure drop is a function of the thermophysical properties of the fluid (i.e. viscosity and density) which, in turn, are temperature dependent. For the sake of simplicity, the analysis presented in this study considers equivalent pipe lengths to include the pressure drops of straight pipes plus all minor pressure drops due to bends, elbows, reducers and tees that could exist through a pipe section. The reader is referred to Ref. [24] for further details.

2.3 | Control valve model

To regulate the mass flow rate through a pipe, a control valve is used. Changes in the flow, in turn, modify the pressure drop in the valve. As in the case for a pump, the theoretical analysis to calculate the pressure drop for a valve is a rather challenging task [24]. To address this issue, a dimensionless parameter obtained experimentally, termed valve's loss coefficient (K_L), is
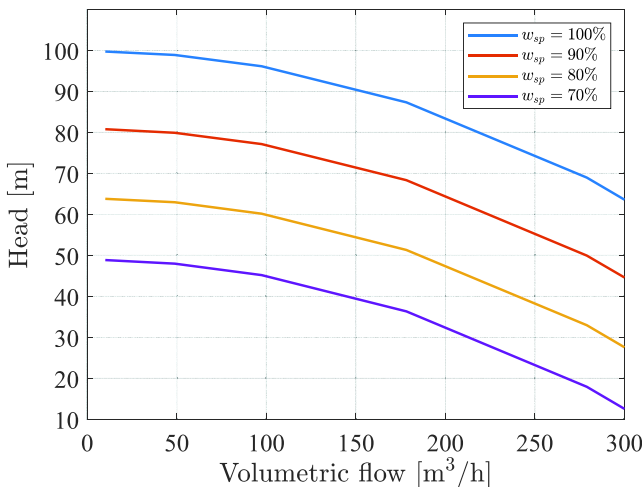

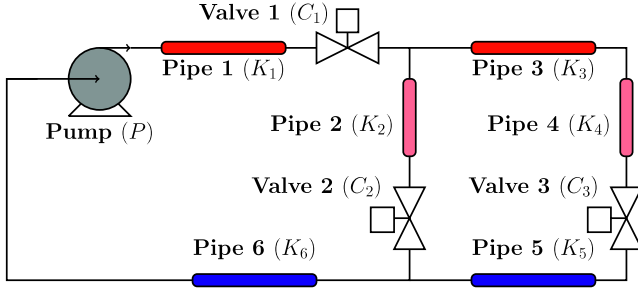**FIGURE 1** Head-flow pump characterisation curves

FIGURE 2 Schematic diagram of a simple pipe network

TABLE 1 Valve's loss coefficient

Opening valve o_v [%]	Valve's loss coefficient K_L [-]
10	194.41
20	48.37
30	21.68
40	12.19
50	7.74
60	5.37
70	4.10
80	3.06
90	2.44
100	2

Note: K_L is a dimensionless quantity [24].

TABLE 2 Parameters of the pump and pipes

Variable	Unit	Value
Pipe diameter (D_{kx})	m	0.2523
Pipe area (A_{kx})	m^2	0.05
Pump's flow area (A_p)	m^2	0.05
ε/D	-	100×10^{-6}
Length pipe 1 (L_{k1})	m	300
Length pipe 2 (L_{k2})	m	5
Length pipe 3 (L_{k3})	m	200
Length pipe 4 (L_{k4})	m	1
Length pipe 5 (L_{k5})	m	200
Length pipe 6 (L_{k6})	m	300
Pump's nominal head	m	50
Motor efficiency (η_m)	-	0.95
Hydraulic efficiency (η)	-	0.93

used instead to analytically describe the relation between the volumetric flow and the pressure drop in the valve. This parameter is typically given by manufacturers and is dependent on the valve opening (o_v). Incorporating K_L, the valve's pressure drop is calculated by

$$\Delta p = \frac{K_L(o_v)\rho v^2}{2}. \tag{8}$$

3 | MODELLING APPROACH OF PIPE NETWORKS

The models presented in Section 2 are amenable to conduct steady-state studies. However, an analysis of the system's dynamic performance upon disturbances is essential to ensure adequate operating conditions and that the energy supply is met.

The hydraulic dynamics of a pipe network are described by the rate of change of flow velocity or volumetric flow rate and pressure drops. Linear momentum and Newton's second law of motion are used to establish a complete model. Linear momentum (M) defines the relation between the total mass (m) and velocity of a fluid (v) as [26,27].

$$M = mv. \tag{9}$$

Newton's second law can be written in terms of momentum as

$$F = \frac{\Delta M}{\Delta t} = m\frac{dv}{dt}. \tag{10}$$

By having a constant cross-sectional area (A_c) and pressure drop (Δp) through the pipe, the total force to accelerate the fluid inside the pipe can be calculated with $F = A_c\Delta p$. The dynamic relationship between the hydraulic variables is then

$$m\frac{dv}{dt} = A\Delta p. \tag{11}$$

For completeness, the model of a simple pipe network, shown in Figure 2, is explained next. It comprises two branches with three valves, six pipes and a pump. Valve 1 is included to protect the system from overpressure. The valve's loss coefficient values are shown in Table 1. These have been obtained directly from information available in Apros. System parameters are summarised in Table 2.

The fluid behaviour in a pipe network may be analysed using an electric analogy. The flow velocity and pressure drop are analogous to current and voltage, respectively. This observation enables to use Kirchhoff's laws to calculate the flow velocity in the branches of the pipe network. For the system in Figure 2, the mathematical model is developed using Equations (3), (7), (8) and (11). The total force in each branch is obtained using the pressure boost/drop and the flow area of each element. The total force should produce a specific acceleration for the total fluid's

mass in the system. Thus, the hydraulic branch velocities are calculated by solving the following equations:

$$m_{t1}\frac{dv_1}{dt} = A_p\Delta p_P - A_{k1}\Delta p_{k1} - A_{c1}\Delta p_{c1}$$
$$- A_{k2}\Delta p_{k2} - A_{c2}\Delta p_{c2} - A_{k6}\Delta p_{k6} \qquad (12)$$

$$m_{t2}\frac{dv_2}{dt} = -A_{k3}\Delta p_{k3} - A_{k4}\Delta p_{k4} - A_{c3}\Delta p_{c3}$$
$$- A_{k5}\Delta p_{k5} + A_{c2}\Delta p_{c2} + A_{k2}\Delta p_{k2} \qquad (13)$$

It should be highlighted that the presented modelling technique is based on the momentum conservation law (9). To verify its suitability for the modelling of pipe networks, the model given by Equations (12) and (13) has been implemented in MATLAB and compared to a model built in Apros. Since Apros considers one-dimensional conservation equations for mass, momentum and energy, such a comparison gives confidence in the modelling approach presented in this work. Simulation results obtained with both software platforms are shown in Figure 3. As it can be observed, flow velocities (top graph) agree on well in both cases. This demonstrates the high accuracy of the presented mathematical model.

Note: It is important to emphasise that although volumetric flow rate (Q) is commonly used in practical projects to describe hydraulic systems, the modelling approach and results presented in this study are specified in terms of fluid velocity and mass flow rate ($\dot{m}$). The rationale behind this choice is that the equations describing the pressure boost or drop of the hydraulic components (pumps, pipes and valves) and the relationship between linear momentum and Newton's second law are given in terms of fluid velocity. Moreover, an electric-hydraulic analogy was adopted, where the fluid velocity is analogous to electric current. On the other hand, mass flow rate is used in Section 4 as the heat consumption P_T in a substation is easily calculated with $P_T = \dot{m}c_p(\Delta T)$, where c_p is the specific heat of the fluid and T is the temperature of the fluid. If required, Q can be easily obtained from fluid velocity using $Q = Av$, where A is the cross-sectional area of the pipe or from mass flow rate using $Q = \dot{m}/\rho$.

4 | CONTROL SYSTEM DESIGN EXAMPLE OF A DHS

A simple pipe network (see Figure 2) was adopted in Section 3 to clearly illustrate the modelling approach introduced in this paper. However, to demonstrate its capabilities for realistic applications, the DHS configuration shown in Figure 4 is adopted in this section. This consists of three substations and one heat source. The supply and return pipelines are numbered from 1 to 3 and from 4 to 6, respectively. A linear control valve and a flat plates heat exchanger (H_{xi}) are used in each substation. The control valve regulates the fluid's mass flow rate in the primary circuit of the heat exchanger. A closed-loop temperature controller is included to ensure a constant

temperature in the secondary circuit despite variations in mass flow rate. This is based on the frequency domain method presented in Refs [28,29] and explained in Appendix A3.

The head-volumetric flow curves of the pump are given in Figure 1. The coefficients in Equation (3) are $P_1 = -0.0004$, $P_2 = 0.0019$ and $P_3 = 99.75$. The diameter and the relative roughness of the pipes are the same for the entire network: $\varepsilon/D = 100 \times 10^{-6}$ and $D = 0.25\ m$.

The pressure drop of the heat exchanger is calculated with [29].

$$\Delta p = \frac{64}{\text{Re}}\frac{\rho v^2}{2D_h}L, \qquad (14)$$

where $D_h = 0.01\ m$ is the hydraulic diameter, $L = 1m$ is the length of the heat exchanger and v is the mean velocity (defined by $v = \dot{m}/\rho A_c$, where $A_c = 0.25\ m^2$ is the cross-sectional area of the heat exchanger for each fluid).

The pump should keep a constant pressure drop in the substation located farthest away from it (in this case, H_{x3}). In a DHS, pressure control is typically achieved by setting the speed of a circulating pump through a controller and by regulating the mass flow rate with an auxiliary valve. This way, the valve in each substation will provide enough mass flow rate of water to guarantee the supply of heat [1]. The minimum differential pressure level required depends on the mass flow rate demand in the substations.

Typically, differential pressure control schemes are based on a look-up table establishing the relationship between the pump speed according to heat demand conditions. Such a relationship is defined by a previous characterisation of the system rather than a dynamic model. To demonstrate the advantages of the dynamic modelling methodology presented in this study, a conventional look-up table-based differential pressure control
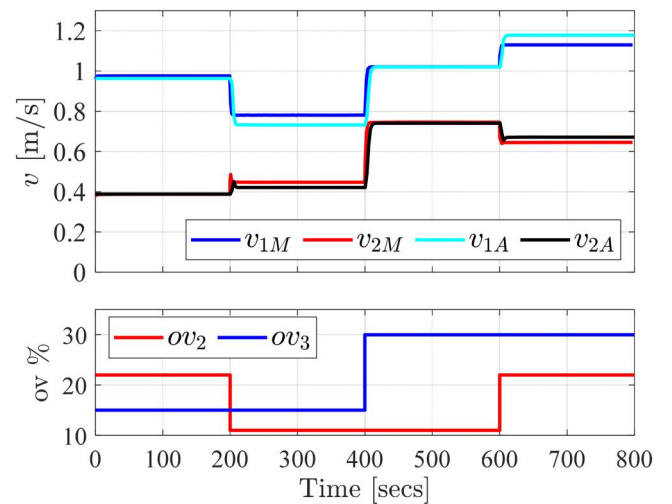

FIGURE 3 Comparison of simulation results of the pipe network. Changes in flow velocities (top graphs) upon variations in valve opening (bottom graphs): results with MATLAB (traces with subscript M) and Apros (traces with subscript A)
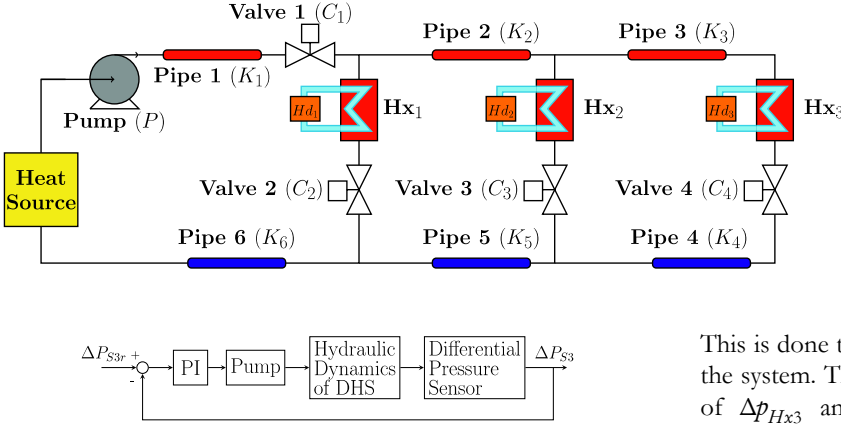
FIGURE 4 Schematic diagram of pipe network of a district heating system

FIGURE 5 Block diagram for a pressure drop-based closed-loop system for the hydraulic dynamics of a district heating system (DHS)

scheme is compared to a pressure drop-based feedback control loop aimed at avoiding inefficient hydraulic performance. Details on the look-up table-based scheme are provided in Section 5, with the remainder of this section dedicated to the control system design of the pressure drop-based scheme.

A schematic of the pressure drop-based feedback control scheme is shown in Figure 5. A PI controller is employed, which is used to maintain a pressure drop reference in the farthest substation (H_{x3}) by regulating the pump speed. The control system design is based on the dynamic model presented in Section 3 using frequency domain tools.

The model capturing the hydraulic dynamic behaviour of the DHS shown in Figure 4 is first obtained. Using Equations (3), (7), (8) and (14), a non-linear differential equation is defined per branch. The system is described by

$$m_{T1}\frac{dv_1}{dt} = \begin{bmatrix} A_p\Delta p_P(\omega_{sp}, v_1) - A_{k1}\Delta p_{k1}(v_1) \\ -A_{c1}\Delta p_{c1}(o_{v1}, v) - A_{H_{x1}}\Delta p_{H_{x1}}(v_1 - v_2) \\ -A_{c2}\Delta p_{c2}(o_{v2}, v_1 - v_2) - A_{k6}\Delta p_{k6}(v_1) \end{bmatrix} \quad (15)$$

$$m_{T2}\frac{dv_2}{dt} = \begin{bmatrix} -A_{k2}\Delta p_{k2}(v_2) - A_{H_{x2}}\Delta p_{H_{x2}}(v_2 - v_3) \\ -A_{c3}\Delta p_{c3}(o_{v3}, v_2 - v_3) - A_{k5}\Delta p_{k5}(v_2) \\ +A_{c2}\Delta p_{c2}(o_{v2}, v_2 - v_1) + A_{H_{x1}}\Delta p_{H_{x1}}(v_2 - v_1) \end{bmatrix} \quad (16)$$

$$m_{T3}\frac{dv_3}{dt} = \begin{bmatrix} -A_{k3}\Delta p_{k3}(v_3) - A_{H_{x3}}\Delta p_{H_{x3}}(v_3) \\ -A_{c4}\Delta p_{c4}(o_{v3}, v_3) - A_{k4}\Delta p_{k4}(v_3) \\ +A_{c3}\Delta p_{c3}(o_{v3}, v_3 - v_2) + A_{H_{x2}}\Delta p_{H_{x2}}(v_3 - v_2) \end{bmatrix} \quad (17)$$

For control design purposes, an additional equation is defined, which calculates the pressure drop in Substation 3.

This is done to use this variable as the mathematical output of the system. The total pressure drop in Substation 3 is the sum of Δp_{Hx3} and Δp_{c3} (i.e. the pressure drops in the heat exchanger and in the valve). The new system variable (Δp_{s3}) is defined as

$$\Delta p_{s3} = \frac{64}{\text{Re}}\frac{\rho L v_3^2}{2D_h} + K_L\frac{\rho v_3^2}{2}. \quad (18)$$

Differentiating Equation (20) with respect to time gives

$$\Delta \dot{p}_{s3} = \left[\frac{64\rho L v_3}{\text{Re}D_h} + K_L\rho v_3\right]\dot{v}_3. \quad (19)$$

The next step is to linearise the system given by Equations (15)–(17) and (19). The state variables are defined as the velocities in each branch and the pressure drop of Substation 3, namely $x_1 = v_1$, $x_2 = v_2$, $x_3 = v_3$ and $x_4 = \Delta p_{s3}$. Using a linearisation method as in Ref. [28], the system is defined by the state-space representation

$$\begin{bmatrix} \Delta\dot{x}_1 \\ \vdots \\ \Delta\dot{x}_4 \end{bmatrix} = \begin{bmatrix} \frac{\partial f_1}{\partial x_1} & \cdots & \frac{\partial f_1}{\partial x_4} \\ \vdots & \ddots & \vdots \\ \frac{\partial f_4}{\partial x_1} & \cdots & \frac{\partial f_4}{\partial x_4} \end{bmatrix}_{x_s} \begin{bmatrix} \Delta x_1 \\ \vdots \\ \Delta x_4 \end{bmatrix} + \begin{bmatrix} \frac{\partial f_1}{\partial u} \\ \vdots \\ \frac{\partial f_4}{\partial u} \end{bmatrix}_{x_s, u_s} [\Delta u],$$

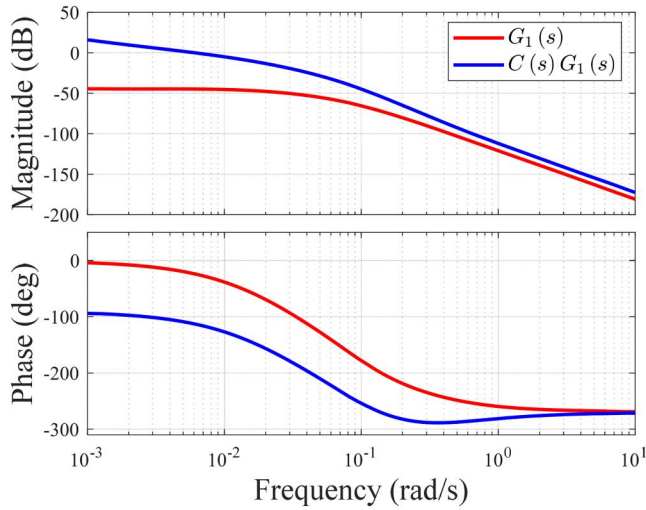$$[\Delta y] = [0\ 0\ 0\ 1]\begin{bmatrix} \Delta x_1 \\ \vdots \\ \Delta x_4 \end{bmatrix}, \quad (20)$$

where $f_n = x_n$ and u is the input of the system. The transfer function $G(s)$ between the output (Δp_{s3}) and the input of the system (pump speed set-point ω_{sp}) is given as

$$\frac{\Delta P_{s3}(s)}{\Omega(s)} = G(s) = C(sI - A)^{-1}B. \quad (21)$$

The linearisation method requires steady-state values (x_s) for specific operating points of the system. In this case, these are defined according to the energy demands. The range of operation is determined by establishing the hydraulic
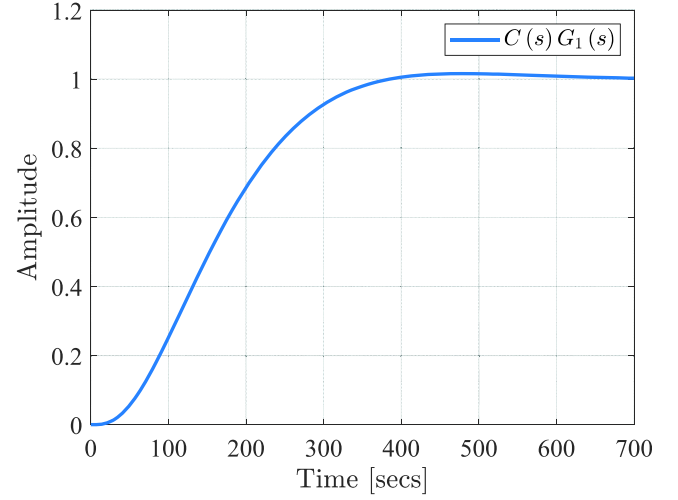
TABLE 3 Steady-state values ($\Delta p_{s3} = 0.5 \times 10^5 Pa$)

| Variable | Heat demands | | | |
	$H_{d1} = 100\%$ $H_{d2} = 100\%$ $H_{d3} = 100\%$	$H_{d1} = 50\%$ $H_{d2} = 100\%$ $H_{d3} = 100\%$	$H_{d1} = 50\%$ $H_{d2} = 50\%$ $H_{d3} = 100\%$	$H_{d1} = 50\%$ $H_{d2} = 50\%$ $H_{d3} = 50\%$
ω_{sp} (%)	72.22	61.37	48.63	34.46
o_{v2} (%)	100	100	100	100
o_{v3} (%)	16.59	6.16	7.14	9.41
o_{v4} (%)	25.33	25.14	9.38	11.23
o_{v5} (%)	32.77	32.93	33.43	12.81
v_1 (m/s)	1.3056	1.0515	0.7955	0.5108
v_2 (m/s)	0.9013	0.9	0.6427	0.3535
v_3 (m/s)	0.4737	0.4759	0.483	0.1854

FIGURE 7 Closed-loop step response

FIGURE 6 Open-loop Bode plot of $G_1(s)$ without controller. Open-loop Bode plot of regulated plant (i.e. $C(s)G_1(s)$)

conditions for the system in Figure 4 during the lowest and highest energy supply demands in each substation. These values are summarised in Table 3 and have been directly obtained from the implementation of the system in Apros. The pressure drop in the farthest substation is defined as 0.5×10^5 Pa, which is the minimum allowable differential pressure for a heat substation [1]. Valve 1 is included for safety purposes only and remains totally open as the pressure drop control is done by the pump.

As discussed previously by the beginning of the section, temperature controllers for each substation in Figure 4 are also implemented in Apros (see Appendices A1-A3 for details). Upon different heat demands, the pump speed is modified to achieve the pressure drop reference in Substation 3.

A family of transfer functions has been obtained for the operating conditions in Table 3. The transfer function representing the system with the highest heat demands, termed $G_1(s)$, is adopted to design the PI controller (see Figure 5). This transfer function is given by

$$G_1(s) = \frac{9.07 \times 10^{-7}}{s^3 + 0.188s^2 + 0.0106s + 1.52 \times 10^{-4}}, \quad (22)$$

where the coefficients with the smallest values have been neglected to avoid numerical instability.

The Bode diagram of $G_1(s)$ is shown in Figure 6, which is used for control system design. The performance specifications are defined as 2% overshoot and a settling time of $t_s = 720$ s. The very small overshoot value is adopted to protect the system against severe variations in pressure drop. The design specifications are translated to the frequency domain as a damping ratio $\zeta = 0.82$, a phase margin $>69°$ and a minimum bandwidth $\omega_{bw} \approx 0.0067$ rad/s. These requirements are met with

$$C(s) = k_p + \frac{k_i}{s} = \frac{2.62s + 1.049}{s}, \quad (23)$$

which is a PI controller designed using Bode shaping techniques. Figure 6 also shows the open-loop Bode diagram of the system once controller (23) is used ($C(s)G_1(s)$). It can be observed that the frequency response specifications are achieved: the system with controller $C(s)$ exhibits a phase margin of 72° and a bandwidth of $\omega_{bw} \approx 0.007$ rad/s. Figure 7 shows the closed-loop step response of the system, showing that the time-domain specifications are satisfactorily met.
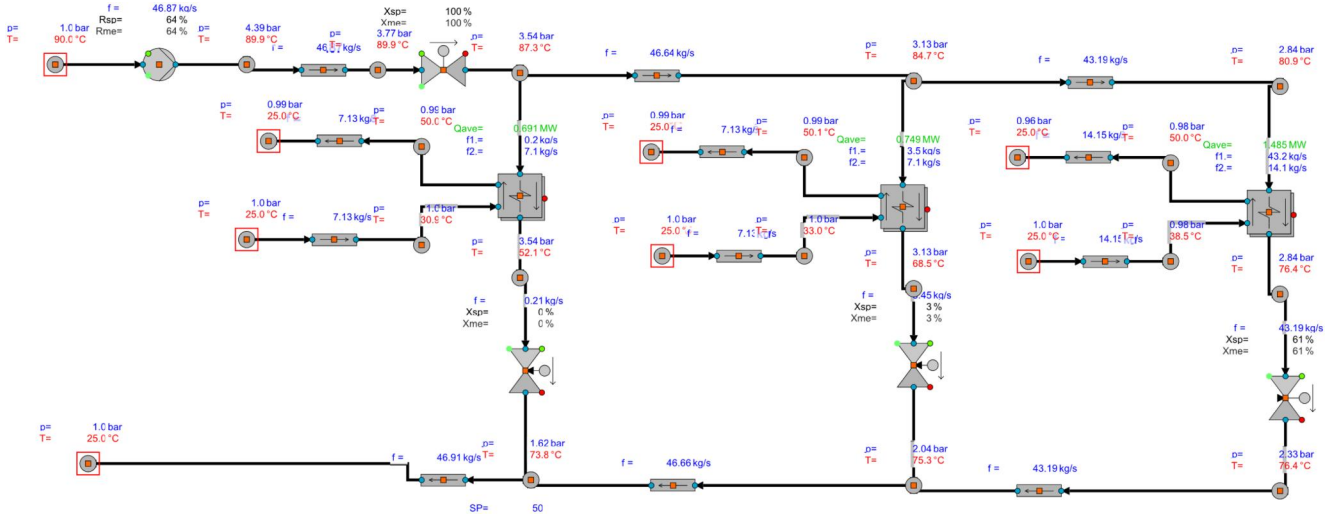
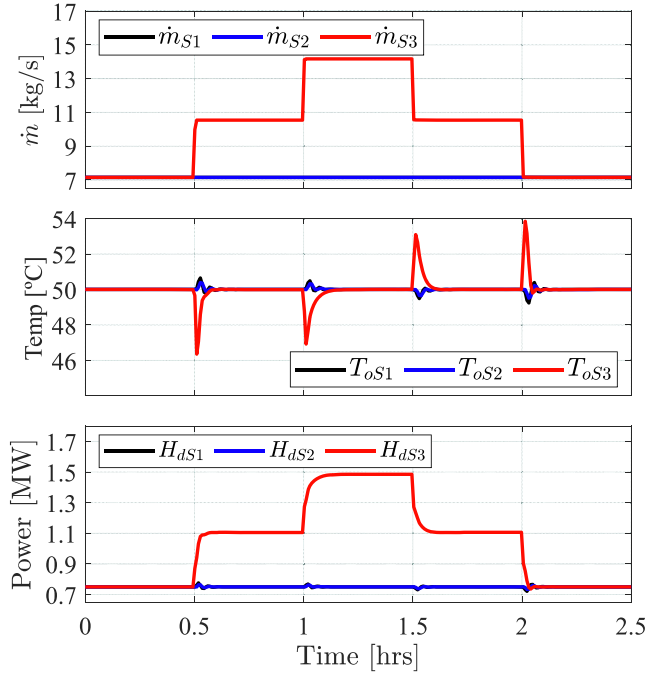**FIGURE 8** Implementation in Apros of the district heating system pipe network

FIGURE 9 Performance of the temperature controller of Substation S3 in Apros

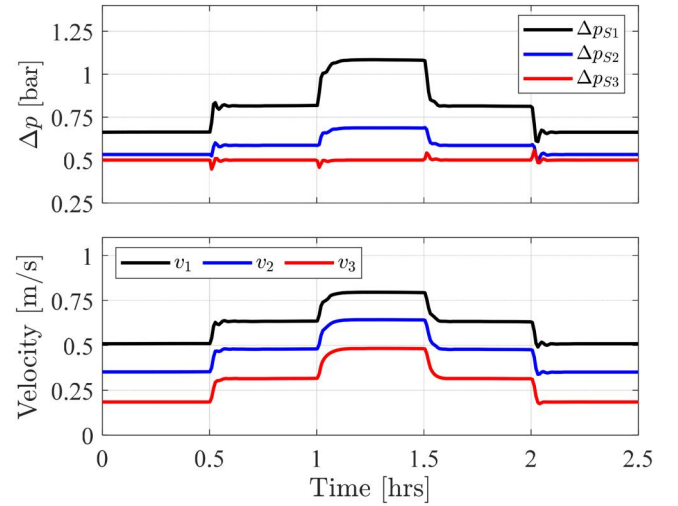**FIGURE 10** System performance (pipe network velocities and substation pressure drops) with presented control strategy

5 | SIMULATION RESULTS AND DISCUSSION

A comparison between the performance of a typical mass flow rate regulation scheme based on a look-up table and the presented control strategy is shown in this section. A screenshot of the system implemented in Apros is shown in Figure 8. Pipes, a flat plates heat exchanger, a pump and control valve elements are used to create the pipe network of the DHS. The controller designed in Section 4 is implemented in Apros by measuring pressure in Substation 3. Then, the controller output is connected to a speed-controlled pump actuator (driver).

Local temperature control in each substation is achieved using a PI controller. This allows to modify the heat demand by increasing the mass flow rate in the secondary circuit of the heat exchanger while maintaining a constant temperature. The substation parameters are given in Appendix A1. The behaviour of temperature, mass flow rate and power consumption upon variations of heat demand is assessed to illustrate the performance of the substations.

System performance is examined first for step changes in heat demand at the farthest substation (H_{dS3}), while heat demand is kept constant in other locations. Three values of H_{dS3} are assessed: 50%, 75% and 100% of the thermal power capacity (equivalent to 0.753, 1.103 and 1.483 MW, respectively). Results are shown in Figures 9–11.

Figure 9 shows the behaviour of the temperature controller. As it can be seen, the output temperature (T_{oSx}) in the consumer circuit (secondary) remains constant
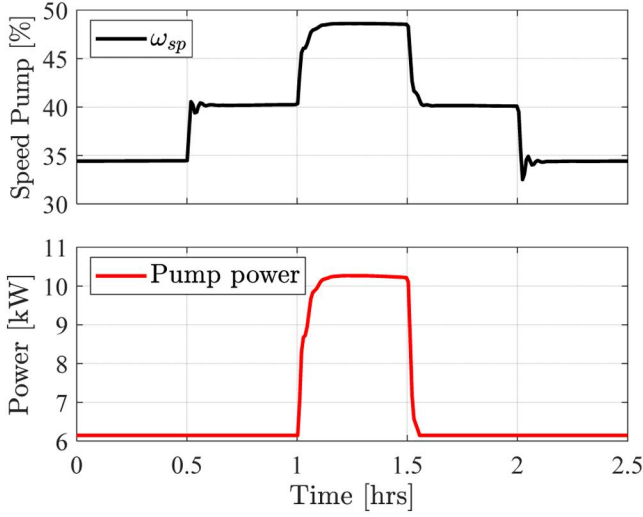
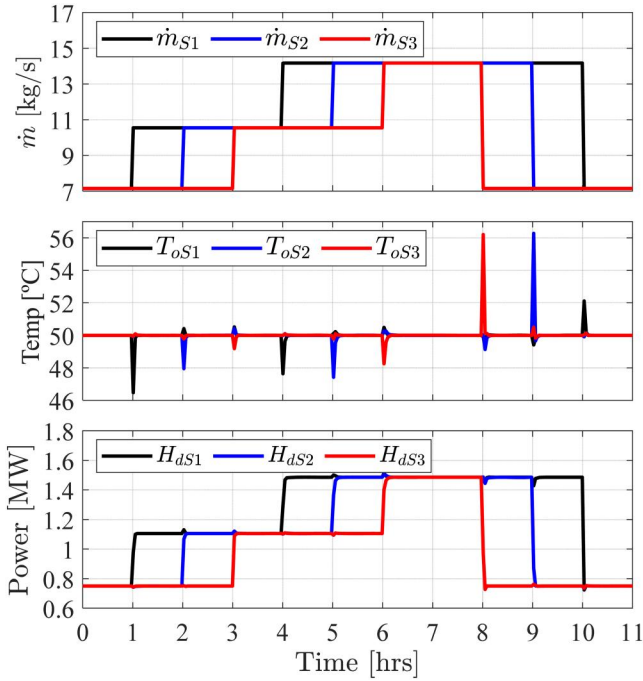**FIGURE 11** Pump speed set-points and power consumption of the pump

FIGURE 12 Substation temperature closed-loop system performance under heat demand changes in all substations

TABLE 4 Look-up table of heat demands and pump speed

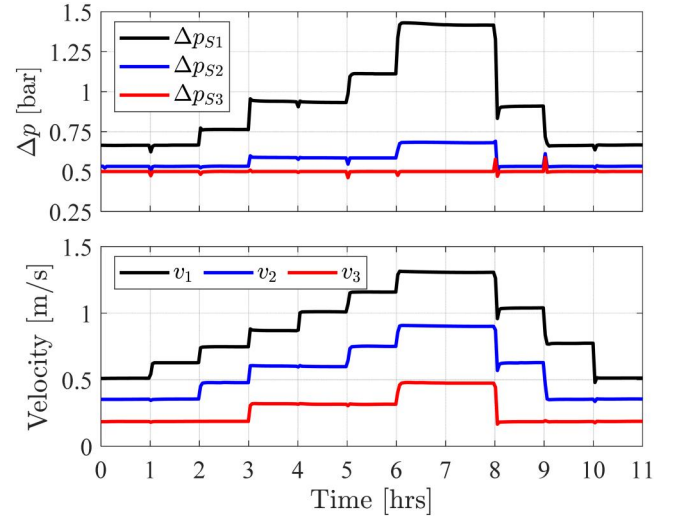| H_{d1} (%)	H_{d2} (%)	H_{d3} (%)	ω_{sp} (%)
50	50	50	35
75	50	50	45
75	75	50	45
75	75	75	50
100	50	50	45
100	75	50	50
100	75	75	55
100	100	50	55
100	100	75	65
100	100	100	75

FIGURE 13 Hydraulic system variable upon heat demand variations

the pressure drop-based control scheme performs well and according with the design specifications defined in Section 4.

Following the initial simulation exercise, more challenging operating conditions are assessed, in which heat demand for all substations is modified. Simulation results are shown in Figures 12 and 13. As it can be observed in Figure 12, the temperature in all substations is successfully regulated to 50°C despite variations in mass flow rate (i.e. heat demand variations). The hydraulic performance of the pressure drop-based controller is shown in Figure 13. As it can be seen, the controller maintains the pressure drop of the farthest away substation (Δp_{s3}) constant irrespectively of changes exhibited by water velocities in pipe branches due to the variations in heat demand at the substations.

To illustrate the superior performance of the presented controller over a conventional implementation, a control strategy using a look-up table to regulate the mass flow rate is implemented in Apros. To ensure a fair comparison, this is assessed with similar operating conditions as in Figures 12 and 13. To achieve this, a look-up table for the set-point of the pump speed
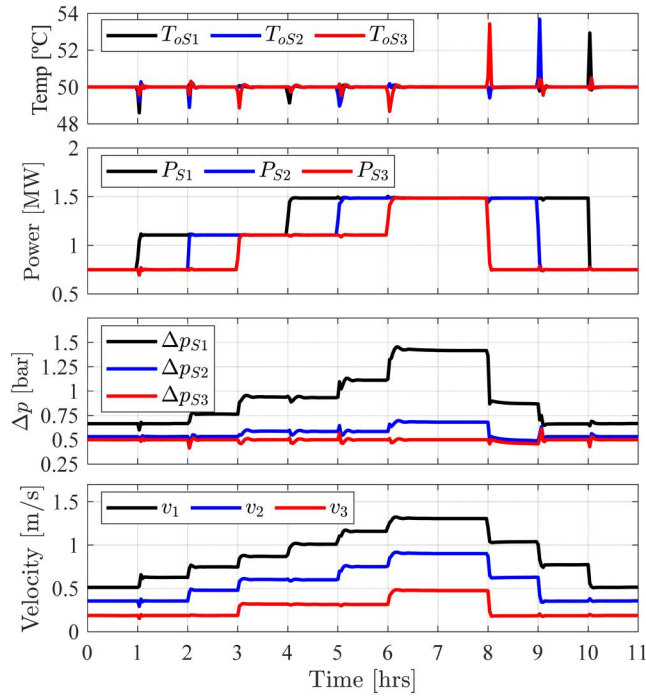
following a short transient upon variations in its mass flow rate ($\dot{m}_{Sx}$).

On the other hand, Figure 10 shows the hydraulic performance of the whole DHS for Substation 3. As it can be observed, the system operates successfully as Δp_{s3} is kept constant despite variations in heat demand.

The pump speed set-point and its power consumption are shown in Figure 11. As it can be observed, the PI controller modifies ω_{sp}, which changes the system pressure to deliver sufficient mass flow rate so as to maintain Δp_{s3} constant. From the results presented in Figures 9 and 10, it can be concluded that

FIGURE 14 Substations and hydraulic system performance when the mass flow rate is regulated by a look-up table
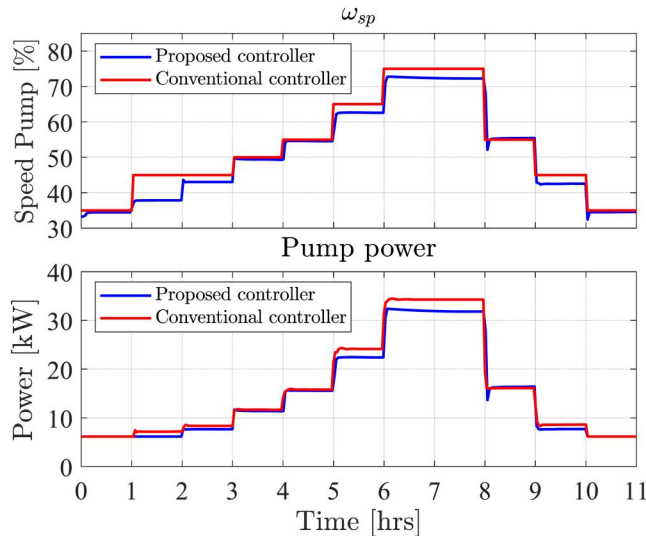

FIGURE 15 Pump speed set-points and power consumption. Comparison between conventional (red trace) and presented (blue trace) control strategies

based on heat demand values is defined to ensure that enough pressure under different demands of mass flow rate is achieved (see Table 4). Results are shown in Figure 14.

Figure 14 shows the performance of the system when the conventional controller is employed. As with the pressure-drop-based control scheme, the system operates well in terms of meeting heat demands: the substation temperature remains constant at 50°C and the heat transfer (power) is similar in both cases (see Figure 12).

To directly compare both control strategies, Figure 15 shows the pump set-points for the different heat demands. When comparing the total power consumption of the pump, this has a value of 0.622 MW when the conventional scheme based on a look-up table is employed—as opposed to 0.588 MW when the presented pressure drop-based control scheme is used. This represents a reduced power consumption of around 5.4%. This power saving may represent a great economic benefit in terms of annual consumption when the pressure drop-based controller is adopted.

Note: It should be emphasised that although the improvement obtained by the modelling, analysis and control approach presented in this study has been demonstrated for a DHS, the methodology is also applicable to a DCS. The level of detail offered by the modelling tools would allow to incorporate different types of fluids employed in DCSs. For instance, thermophysical properties of refrigerants may be included not only for the hydraulic system model, but also for the heat exchanger model in the substations (see Appendices A1-A2).

6 | CONCLUSION

In this study, a dynamic modelling approach for pipe networks based on fluid mechanics concepts was presented. The models afforded by the approach are comprehensive as they consider key parameters such as the friction factor or loss coefficients—often overlooked or considered static in steady-state models. The models are suitable for control system design: following a linearisation exercise, transfer functions were obtained for different operating conditions and a feedback controller for pump speed was designed to ensure a constant pressure drop was kept in the substation farthest away from the pump. Its implementation was carried out in Apros—a commercial software enabling the simulation of DHS with built-in blocks.

Simulation results show that a better performance can be achieved using the presented control strategy compared to a conventional mass flow rate controller based on a look-up table. This is relevant as the hydraulic conditions of the pipe network are maintained, albeit with a reduced power consumption of the pump. Although the conventional strategy does not need the knowledge of key parameters or a dynamic model, it requires the characterisation of the system, which in turn may translate into long commissioning periods. This issue is avoided with the presented scheme.

The developed model considers all parameters involved in the hydraulic behaviour of a DHS. It also allows to go further in the analysis of more complex systems. Given that parameters such as the friction factor or variables such as the water temperature of the heat source can be established in terms of uncertainty, the models could be further used to perform robustness analyses (in a control systems context)—going beyond the model capabilities reported in the open literature.

ORCID

Carlos E. Ugalde-Loo https://orcid.org/0000-0001-6361-4454

REFERENCES

1. Frederiksen, S., Werner, S.: District heating & cooling. Studentlitteratur AB, Lund (2013)
2. Vandermeulen, A., van der Heijde, B., Helsen, L.: Controlling district heating and cooling networks to unlock flexibility: a review. Energy. 151, 103–115 (2018)
3. Wang, D., et al.: Optimal scheduling strategy of district integrated heat and power system with wind power and multiple energy stations considering thermal inertia of buildings under different heating regulation modes. Appl Energy. 240, 341–358 (2019)
4. Yan, A., et al.: Hydraulic performance of a new district heating systems with distributed variable speed pumps. Appl Energy. 112, 876–885 (2013)
5. Sheng, X., Lin, D.: Electricity consumption and economic analyses of district heating system with distributed variable speed pumps. Energy Build. 118, 291–300 (2016)
6. Sheng, X., Lin, D.: Energy saving analyses on the reconstruction project in district heating system with distributed variable speed pumps. Appl. Therm. Eng. 101, 432–445 (2016)
7. Wang, H., Wang, H., Zhu, T.: A new hydraulic regulation method on district heating system with distributed variable-speed pumps. Energy Convers. Manag. 147, 174–189 (2017)
8. Sheng, X., Lin, D.: Energy saving factors affecting analysis on district heating system with distributed variable frequency speed pumps. Appl. Therm. Eng. 121, 779–790 (2017)
9. Ateş, S.: Hydraulic modelling of closed pipes in loop equations of water distribution networks. Appl. Math. Model. 40(2), 966–983 (2016)
10. Ateş, S.: Hydraulic modelling of control devices in loop equations of water distribution networks. Flow Meas. Instrum. 53, 243–260 (2017)
11. Gong, E., et al.: Optimal operation of novel hybrid district heating system driven by central and distributed variable speed pumps. Energy Convers. Manag. 196, 211–226 (2019)
12. Gu, J., et al.: Analysis of a hybrid control scheme in the district heating system with distributed variable speed pumps. Sustain. Cities Soc. 48, 1–10 (2019)
13. Jing, Z.X., et al.: Modelling and optimal operation of a small-scale integrated energy based district heating and cooling system. Energy. 73, 399–415 (2014)
14. Wang, Y.-F., Chen, Q.: A direct optimal control strategy of variable speed pumps in heat exchanger networks and experimental validations. Energy. 85, 609–619 (2015)
15. Pan, Z., Guo, Q., Sun, H.: Interactions of district electricity and heating systems considering time-scale characteristics based on quasi-steady multi-energy flow. Appl Energy. 167, 230–243 (2016)
16. Oppelt, T., et al.: Dynamic thermo-hydraulic model of district cooling networks. Appl. Therm. Eng. 102, 336–345 (2016)
17. Wang, H., et al.: Optimization modeling for smart operation of multi-source district heating with distributed variable-speed pumps. Energy. 138, 1247–1262 (2017)
18. Viljoen, J.H., Muller, C.J., Craig, I.K.: Dynamic modelling of induced draft cooling towers with parallel heat exchangers, pumps and cooling water network. J. Process Contr. 68, 34–51 (2018)
19. Wang, H., Meng, H.: Improved thermal transient modeling with new 3-order numerical solution for a district heating network with consideration of the pipe wall's thermal inertia. Energy. 160, 171–183 (2018)
20. Stennikov, V.A., Barakhtenko, E.A., Sokolov, D.V.: A methodological approach to the determination of optimal parameters of district heating systems with several heat sources. Energy. 185, 350–360 (2019)
21. del Hoyo Arce, I., et al.: Models for fast modelling of district heating and cooling networks. Renew. Sustain. Energy Rev. 82, 1863–1873 (2018)
22. Chapaloglou, S., et al.: Smart energy management algorithm for load smoothing and peak shaving based on load forecasting of an island's power system. Appl. Energy. 238, 627–642 (2019)
23. Bany Ata, A., et al.: Comparison and validation of three process simulation programs during warm start-up procedure of a combined cycle power plant. Energy Convers. Manag. 207, 112547 (2020)
24. Munson, B.R., et al.: Fundamentals of fluid mechanics, 7th ed. John Wiley & Sons, Hoboken (2012)
25. Swamee, P.K., Jain, A.K.: Explicit equations for pipe-flow problems. J. Hydraul. Div. 102, 657–664 (1976)
26. Ogata, K.: System dynamics, 4th ed. Pearson, Upper Saddle River (2013)
27. Kundu, P.K., Cohen, I.M., Dowling, D.R.: Fluid mechanics, 5th ed. Academic Press, San Diego (2011)
28. Bastida, H., et al.: Dynamic modeling and control of a plate heat exchanger. In: Proc. IEEE Conf. Energy Internet and Energy System Integration (EI2), Beijing, China, pp. 1–6 (November 2017)
29. Bastida, H., et al.: Dynamic modelling and control of counter-flow heat exchangers for heating and cooling systems. In: 2019 54th International Universities Power Engineering Conference (UPEC), pp. 1–6 (2019)

APPENDIX A1

The type of heat exchanger used in this study for each sub-station is a flat plates type, with parameters provided in Table A1. Its mathematical model is described by a set of nonlinear differential equations, which are obtained by applying energy balance. This analysis requires a control volume, which is obtained by mathematically representing the heat exchanger by defining a number of nodes. Figure A1 shows such a division process for three nodes. According to Ref. [26], this amount of nodes provides an adequate model suitable for the design of PI-based temperature controllers.

TABLE A1 Heat exchanger parameters

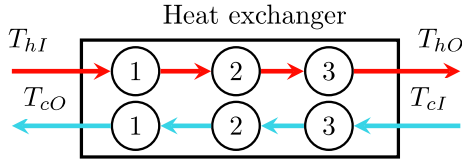| Variable	Unit	Value
Gap (g)	mm	5
Plate length (P_L)	m	1
Plate width (P_W)	m	1
Number of plates (N_P)	-	100
Hot volumetric capacity (V_h)	m^3	0.25
Cold volumetric capacity (V_c)	m^3	0.25
Total heat transfer area (A_t)	m^2	200
Hydraulic diameter (D_h)	mm	5
Plate thickness (b_{fp})	mm	1
Plate material thermal conductivity (k_{fp})	W/m°C	50

Heat exchanger

FIGURE A1   Three nodes division of the heat exchanger

APPENDIX A2

The thermal dynamic behaviour of the hot and cold streams in each node is described by a pair of non-linear differential equations per node:

$$\dot{T}_{h1} = \dot{x}_1 = \left(\dot{m}_h c_{ph1}(T_{hI} - x_1) + U_1 A_t(x_2 - x_1) \right) \Big/ m_{hc} c_{ph1},$$
(24)

$$\dot{T}_{c1} = \dot{x}_2 = \left(\dot{m}_c c_{pc1}(x_4 - x_2) + U_1 A_t(x_1 - x_2) \right) \Big/ m_{hc} c_{pc1},$$
(25)

$$\dot{T}_{h2} = \dot{x}_3 = \left(\dot{m}_h c_{ph2}(x_1 - x_3) + U_2 A_t(x_4 - x_3) \right) \Big/ m_{hc} c_{ph2},$$
(26)

$$\dot{T}_{c2} = \dot{x}_4 = \left(\dot{m}_c c_{pc2}(x_6 - x_4) + U_2 A_t(x_3 - x_4) \right) \Big/ m_{hc} c_{pc2},$$
(27)

$$\dot{T}_{h3} = \dot{x}_5 = \left(\dot{m}_h c_{ph3}(x_3 - x_5) + U_3 A_t(x_6 - x_5) \right) \Big/ m_{hc} c_{ph3},$$
(28)

$$\dot{T}_{c3} = \dot{x}_6 = \left(\dot{m}_c c_{pc3}(T_{cI} - x_6) + U_3 A_t(x_5 - x_6) \right) \Big/ m_{hc} c_{pc3},$$
(29)

where T_x is the temperature in each heat exchanger node, $\dot{m}_h$ and $\dot{m}_c$ are the mass flow rates of the hot and cold stream, respectively, c_{px} is the specific heat, U is the heat transfer coefficient and A_t is the heat transfer area. Further details on the calculation of U are provided in Ref. [26]. Thus, the temperature output of the hot and the cold streams are $T_{hO} = x_5$ and $T_{cO} = x_2$, respectively.

System Equations (24)–(29) are linearised using the Taylor series expansion method. The linear state-space system

$$\begin{bmatrix} \Delta\dot{x}_1 \\ \vdots \\ \Delta\dot{x}_6 \end{bmatrix} = \begin{bmatrix} \dfrac{\partial f_1}{\partial x_1} & \cdots & \dfrac{\partial f_1}{\partial x_6} \\ \vdots & \ddots & \vdots \\ \dfrac{\partial f_6}{\partial x_1} & \cdots & \dfrac{\partial f_6}{\partial x_6} \end{bmatrix}_{x_s} \begin{bmatrix} \Delta x_1 \\ \vdots \\ \Delta x_6 \end{bmatrix} + \begin{bmatrix} \dfrac{\partial f_1}{\partial u} \\ \vdots \\ \dfrac{\partial f_6}{\partial u} \end{bmatrix}_{u_s} [\Delta u],$$

TABLE A2   Steady-state values

Cells	U (W/m²°C)	c_p (J/kg°C)	$T = x$ (°C)
Hot stream (1)	225.3003	4195.7	77.7203
Cold stream (1)		4181.3	49.9998
Hot stream (2)	207.6160	4188	66.9268
Cold stream (2)		4178.7	40.5555
Hot stream (3)	191.3234	4178	32.2745
Cold stream (3)		4178	32.2745

$$[\Delta y] = [\, 0 \quad 1 \quad 0 \quad 0 \quad 0 \quad 0 \,] \begin{bmatrix} \Delta x_1 \\ \vdots \\ \Delta x_6 \end{bmatrix},$$
(30)

is obtained, where $f_n = x_n$, u is the system input, which is the mass flow rate of the hot stream ($\dot{m}_h$) and the system output y is the outlet cold stream temperature (x_2). The state-space system (30) is represented as a transfer function using

$$Y(s)/U(s) = G(s) = \mathbf{C}(sI - \mathbf{A})^{-1}\mathbf{B}.$$
(31)

The linearisation method requires steady-state values (x_s) for a specific operating point to calculate Equation (31). The operating point used to design the controller for a substation is established for a maximum mass flow rate of the consumer circuit (cold stream) of $\dot{m}_c = 15$ kg/s and a temperature output set-point of $T_{c1} = x_2 = 50$°C. The input temperature of the hot stream (heat source) is established as $T_{hI} = 90$°C and the input temperature of the cold stream as $T_{cI} = 25$°C. Being proportional control volumes, each node has the same heat transfer area and total mass of water: $A_{tx} = 66.67$ m² and $m_{hcx} = 166.57$ kg. The steady-state values under these conditions are shown in Table A2.

APPENDIX A3

Using Table A2, Equations (30) and (31), the following transfer function is obtained:

$$G(s) = \frac{\begin{matrix} 0.0017s^4 + 0.00084s^3 + 1.96 \times 10^{-4}s^2 \\ + 2.14 \times 10^{-5} + 9.15 \times 10^{-7}s \end{matrix}}{\begin{matrix} s^6 + 0.63s^5 + 0.164s^4 + 0.023s^3 + 0.0017s^2 \\ + 6.9 \times 10^{-5}s + 1.1 \times 10^{-6} \end{matrix}}$$
(32)

The dynamic behaviour of the control valve used to regulate the input ($\dot{m}_h$) should be considered in the control design process. The valve opening (o_v) and the mass flow rate ($\dot{m}_h$) through the valve is defined by
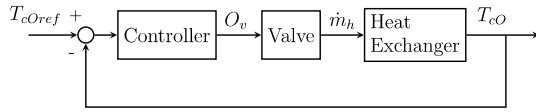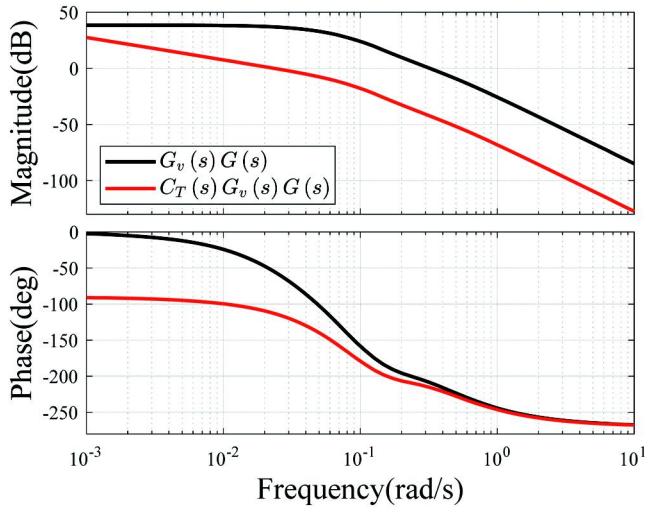
$$G_v(s) = \frac{100}{3s + 1}$$
(33)

A block diagram of the feedback control scheme is shown in Figure A2. Frequency domain tools are employed to design a closed-loop controller for the system given by Equations (32) and (33). The desired performance requirements of the system are a settling time $t_s = 180$ s and a maximum overshoot of 5%, which in the frequency domain translate to a damping ratio $\zeta = 0.69$, a phase margin of at least 64.6° and a minimum bandwidth $\omega_{bw} = 0.03\, rad/s$.
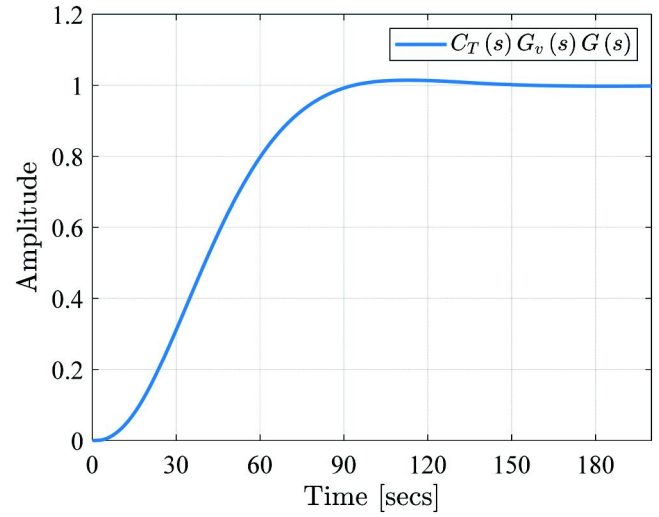
Bode shaping techniques are used to meet the desired specifications. These are achieved by the following PI controller:

$$C_T(s) = k_p + \frac{k_i}{s} = \frac{0.007514s + 0.0002852}{s} \qquad (34)$$

As shown by the open-loop Bode diagrams of the system with and without controller in Figure A3, a phase margin of 67° and a bandwidth $\omega_{bw} = 0.03$ rad/s are obtained once the controller is in place. The step response of the closed-loop system is shown in Figure A4. As it can be observed, the specifications in the time and frequency domain are clearly met.